Regional changes in choroidal thickness associated with accommodation

Emily C. Woodman-Pieterse, Scott A. Read, Michael J. Collins, David Alonso-Caneiro

Affiliation for all authors: Contact Lens and Visual Optics Laboratory, School of Optometry and Vision Science, Queensland University of Technology, Brisbane, Queensland, Australia

Corresponding Author: Emily Woodman-Pieterse, Contact Lens and Visual Optics Laboratory, School of Optometry and Vision Science, Queensland University of Technology, Room B556, O Block, Victoria Park Road, Kelvin Grove 4059, Brisbane, Australia; e.woodman@qut.edu.au

Word count: 4622

Number of Figures: 5

Number of Tables: 2

Date of Submission: 24/08/15

Abstract

Purpose: To characterise the changes occurring in choroidal thickness (ChT) across the posterior pole during accommodation using enhanced-depth imaging optical coherence tomography (OCT).

Methods: Forty participants (mean age 21 ± 2 years) had measures of ChT and ocular biometry taken during accommodation to 0, 3 and 6 dioptre (D) stimuli, with the Spectralis OCT and Lenstar biometer. A Badal optometer and cold mirror system was mounted on both instruments, allowing measurement collection while subjects viewed an external fixation target at varying accommodative demands.

Results: The choroid exhibited significant thinning during accommodation to the 6 D stimulus in both subfoveal (mean change −5 ± 7 μm) and parafoveal regions ($p < 0.001$). The magnitude of these changes varied by parafoveal meridian, with the largest changes seen in the temporal (−9 ± 12 μm) and inferotemporal (−8 ± 8 μm) meridians ($p < 0.001$). Axial length increased with accommodation (mean change +5 ± 11 μm at 3 D, +14 ± 13 μm at 6 D) and these changes were weakly negatively associated with the choroidal changes ($r^2 = 0.114$, $p < 0.05$).

Conclusions: A small, but significant thinning of the choroid was observed at the 6 D accommodation demand, which was greatest in the temporal and inferotemporal parafoveal choroid, and increased with increasing eccentricity from the fovea. The regional variation in the parafoveal thinning corresponds to the distribution of the nonvascular smooth muscle within the uvea, which may implicate these cells as the potential mechanism by which the choroid thins during accommodation.

Introduction

Alterations in axial length are the major structural change underlying the development and progression of refractive error,[1-3] however there is also evidence supporting an involvement of the choroid in refractive error development.[4-9] Animal studies experimentally inducing refractive error, show that rapid changes in choroidal thickness (ChT) appear to precede the longer term eye growth changes associated with the development of myopia and hyperopia.[6, 7] When myopia development is induced it is characterised by a rapid choroidal thinning, followed by longer term increases in eye growth, whereas when hyperopia is induced choroidal thickening, followed by a slowing of eye growth occurs. Recent cross-sectional human studies in both adults[8-11] and children[5] indicate that longer term ChT changes also appear to accompany refractive error development in humans, with a thinner choroid associated with increased axial length and myopia. Collectively, these data suggest that changes in ChT may reflect one of the early signals associated with changes in ocular growth and refractive error development.

Due to the proposed link between near work and myopia,[12-17] numerous studies have examined the way in which various ocular parameters change during accommodation.[18-24] Along with the well documented changes in anterior eye biometrics,[18] a number of recent studies have reported significant increases in axial length to accompany accommodation.[19-24] Using optical low coherence reflectometry (OLCR) we have previously reported some evidence of a small but significant thinning of the subfoveal choroid during accommodation, that was weakly negatively associated with the observed axial elongation.[23]

However, the use of OLCR to assess ChT in our previous study was a limitation, since the determination of ChT requires subjective judgement, and was only possible in 63% of subjects with this technique. Additionally, these measurements only represented ChT at the subfoveal location at a single accommodation demand (4 D), which provided no information about the regional variations in ChT with accommodation, or the relationship between the magnitude of choroidal response and the accommodation demand.

In this study we use the higher resolution technique of optical coherence tomography (OCT) to provide a better understanding of the ChT changes associated with accommodation at 0, 3 and 6 D demands. Furthermore, OCT also allows measures of regional changes in ChT across the posterior pole that may provide greater insight into the mechanism underlying the change, rather than examining just a single subfoveal location. This experiment therefore aimed to comprehensively characterise the regional ChT response to a range of accommodation demands using OCT in a population of young adult myopes and emmetropes.

Methods

Subjects

Forty healthy young adult participants, aged 18-25 years (mean 21 ± 2 years), were recruited from the students of the Queensland University of Technology. Approval from the University Human Research Ethics Committee was obtained before commencement of the study, and subjects gave written informed consent to

participate. All subjects were treated in accordance with the tenets of the Declaration of Helsinki.

Prior to testing, subjects were screened to identify and exclude those with any history of significant systemic or ocular disease, injury or surgery. Any subject who identified as a cigarette smoker was also excluded from the study, due to the reported choroidal thinning associated with cigarette smoking.[25] Subjects initially underwent an eye examination to determine their refractive, visual and binocular vision status. All subjects were required to have best corrected visual acuity of logMAR 0.00 or better and amplitudes of accommodation in excess of 6 D. Those who routinely used soft contact lenses refrained from lens wear for at least 24 hours prior to testing (n = 16), and no rigid contact lens wearers were included in the study.

Subjects were classified according to their subjective non-cycloplegic spherical equivalent refraction (SER) as either emmetropic (n = 20, SER −0.25 - +0.75 D, cylinder ≤ 1 DC; mean SER +0.38 ± 0.22 D, mean cylinder −0.25 ± 0.2 DC) or myopic (n = 20, SER −0.75 - −6.00 D, cylinder ≤ 1 DC; mean SER −2.83 ± 1.50 D, mean cylinder −0.35 ± 0.3 DC). These groups were well matched in terms of age (emmetropes 21 ± 1 years, myopes 22 ± 2 years), gender (each group comprised of 50% female, 50% male) and monocular amplitude of accommodation (emmetropes 11 ± 1 D, myopes 11 ± 2 D).

Instrumentation

Following the screening and classification of participants, each subject had measures of the ChT, retinal thickness (RT), and axial ocular dimensions of their left

eye collected, during various levels of accommodation. Cross-sectional chorio-retinal images allowing determination of ChT and RT were obtained with the Heidelberg Spectralis (Heidelberg Engineering, Heidelberg, Germany) spectral domain OCT (SD-OCT) using the enhanced depth imaging mode to optimise the visibility of the choroid.[26] Axial ocular dimensions were acquired using the Lenstar LS900 optical biometer (Haag-Streit AG, Koeniz, Switzerland) which provides measures of central corneal thickness (CCT), anterior chamber depth (ACD), lens thickness (LT), and axial length (AL). A Badal optometer and cold mirror system that could be mounted on both the OCT and optical biometer was custom built in order to allow measurements to be collected while an external fixation target (an LCD screen from an iPhone 4S, Apple Inc., California, USA) was viewed simultaneously with varying accommodation demands (Figure 1). The Badal optometer was used to correct any spherical ametropia (best sphere correction) for each subject, and to provide a 0, 3 or 6 D accommodation stimulus. The subjects' right eyes were occluded for the duration of the experiment to eliminate the potential confounding effects of convergence in the eye being measured.

To ensure measurements obtained with the biometer and OCT were not affected by the presence of the cold mirror, five subjects had measurements taken with and without the mirror in place with both instruments. The mean difference values between the repeated measures of axial biometry, subfoveal ChT and foveal RT were 1 micron or less, indicating excellent agreement between the measurements with and without the cold mirror for all parameters. No significant change in the average OCT image quality index (QI) score was found with the cold mirror in place.

Procedure

Prior to any measurements, participants were required to watch a movie on the LCD screen (screen resolution 326 ppi, screen luminance approximately 20 cd/m^2) imaged at infinity through the Badal system for 10 minutes to wash out any effects of previous near work. The movie was then paused and a 49 x 49 mm, high-contrast Maltese cross target was presented on the screen. The subject was instructed to fixate with their left eye on the centre of the Maltese cross target adjacent to the instrument's fixation light and to keep it in sharp focus for the duration of the measurement. Two measurements were taken on the left eye of each subject with the OCT at each accommodation level, with each measurement consisting of a high resolution (1536 x 496 pixels per B-scan) six-line radial "star" scan centred on the fovea. Each line scan was 30° wide and consisted of the average of 30 B-scans. All collected scans had a QI score of ≥ 25 dB (mean QI of all scans was 34.1 ± 4.7 dB). The extra-long ("XL") eye length setting was used for all subjects, regardless of axial length to allow enough space between the instrument and the subject's fixating eye for the cold mirror. The initial baseline measurement (0 D stimulus) was set as the reference scan, and all subsequent scans were registered to the same retinal location using the instrument's "auto-rescan" feature.

After the baseline images were obtained, the fixation target was reverted back to the movie on the LCD screen, but this time the screen was positioned to provide a 3 D stimulus to accommodation. The subjects continued this accommodation task for 10 minutes before the movie was again paused, the Maltese cross fixation target was presented, and measurements were taken. The subjects then returned to their movie viewing for another 10 minute wash out period with the Badal system imaged at infinity. The LCD screen was then moved to provide a 6 D stimulus for 10

minutes, and measurements were once again taken. The same protocol was also carried out with the Badal system mounted on the Lenstar biometer and five measurements were taken on the left eye of each subject and averaged at each accommodation stimulus level.

The task duration was determined from our previous findings that changes in ChT were at a maximum about 10 minutes after commencing accommodation, and that both AL and ChT had returned to baseline levels within 10 minutes of task completion.[22] To reduce the potential confounding influence of diurnal variation in ocular parameters,[27-29] measurement sessions were restricted to 0800-1200 hours each day. The order of instrument measurements was randomised for each subject to eliminate any order effects, and data from both the instruments was collected on the same day.

Data Analysis

The OCT images were exported and analysed using custom written software. Each scan was initially segmented using an automated algorithm, delineating the inner limiting membrane (ILM) and the outer surface of the retinal pigmented epithelium (RPE) to determine RT, and the RPE and the inner surface of the chorio-scleral interface to determine the ChT, across the full 30° width of the scan.[30] One experienced observer, masked to the subjects' refractive error and accommodation level then checked the integrity of the automated segmentation, and manually corrected any errors. The two segmented scans taken at each accommodation level were then averaged to provide the mean RT and ChT across the six radial scans at the 0, 3 and 6 D demands for each subject.

To account for the influence of ocular magnification in OCT imaging (associated with AL and ocular refraction for each accommodation level), the transverse scale of the scans were adjusted using each subject's refractive data and ocular parameters obtained with the biometer at each accommodation level, using methods previously described.[5] The segmented OCT data were used to derive subfoveal choroidal thickness (SFChT) and foveal RT, along with parafoveal choroidal and retinal thickness maps over a 5 mm diameter.

Repeatability of the imaging and measurement procedures were assessed through Bland-Altman[31] analysis of the two repeated measures at each session, which revealed a mean difference of −0.5 ± 3.9 μm between the two measures of SFChT per accommodation level, and −0.3 ± 1.9 μm between the two foveal RT measures per accommodation level. Based on the observed within-session repeatability, for our sample size of 40 subjects it was calculated that our study had 80% power to detect a 3 μm change in ChT (and 2 μm change in RT) at the 0.05 level. The mean absolute error (± SD) between the manually corrected and fully automatic segmentation was also calculated for each OCT scan, indicating that the ILM (0.3 ± 1 μm) and RPE (0.9 ± 3 μm) rarely needed manual correction, whereas correction of the chorio-scleral boundary (17 ± 30 μm) was more often required.

To account for the error induced in the AL measurements associated with the increased optical path length of the accommodating eye,[32] each subject's AL measures were adjusted based on their individual biometric measurements obtained with the Lenstar, by methods previously described.[21, 23]

Of the 40 subjects examined, five were excluded from analysis of the parafoveal choroid and retina (4 emmetropes, 1 myope). Two subjects had peripheral portions

of the image of the outer choroidal boundary cut off posteriorly, two subjects were unable to fixate steadily enough to have all six scans captured for all conditions, and one subject had a large portion of their images obscured by the shadow cast on the retina by the edge of the cold mirror. For all other parameters, including foveal RT and SFChT, all 40 subjects were included in the analysis.

Statistical Analysis

A repeated measures ANOVA was performed to examine the changes in SFChT, foveal RT and ocular biometry (CCT, ACD, LT, AL) with accommodation to 0, 3 and 6 D stimuli (within-subject factor), and to observe any differences between refractive groups (between-subject factor). The average parafoveal ChT and RT was calculated for 8 meridians: superior, inferior, nasal, temporal, superonasal, superotemporal, inferonasal and inferotemporal, within three concentric annuli of eccentricities of 1, 3 and 5 mm centred on the fovea (Figure 2). A repeated measures ANOVA was performed for the parafoveal ChT and RT changes, with accommodation level, meridian and eccentricity as within subject factors; and a between subject factor of refractive error group. If significant differences were identified in the main ANOVA ($p < 0.05$), post-hoc testing with Bonferroni correction was performed. ANCOVA was also used to find any associations between the changes in ocular parameters with accommodation, using the methods of Bland and Altman for the analysis of repeated measures.[33]

Results

SFChT decreased significantly ($p < 0.001$) during accommodation (Figure 3). The mean change in SFChT for all subjects ($n = 40$) was −2 ± 6 μm for the 3 D demand, and −5 ± 7 μm for the 6 D demand, however only the change with 6 D was significantly different from baseline ($p < 0.001$). The myopic subjects on average thinned by −1 ± 6 μm at the 3 D demand and −4 ± 8 μm at the 6 D demand, which was not significantly different to the changes seen in the emmetropes at 3 D (−2 ± 7 μm) or 6 D (−5 ± 6 μm) ($p = 0.614$). However, the average baseline SFChT was significantly thinner in the myopes (303 ± 58 μm) compared to the emmetropes (373 ± 77 μm) ($p < 0.05$).

For all subjects with complete parafoveal data ($n = 35$) the mean ChT across the full 5 mm exhibited a highly significant within-subjects main effect of accommodation ($p < 0.001$). Pairwise comparisons showed that it was only at the higher accommodation demand (6 D) that the parafoveal change was significantly different from baseline values (mean change across all meridians and eccentricities −5 ± 12 μm, $p < 0.001$) (Figure 4). A significant main effect of meridian was found ($p < 0.05$), and the accommodation-meridian interaction approached significance ($p = 0.079$), with the greatest changes seen within the temporal (−9 ± 12 μm), inferotemporal (−8 ± 8 μm) and inferior (−6 ± 8 μm) meridians with accommodation to the 6 D demand (Table 1, all $p < 0.001$). Smaller statistically significant changes were also seen within the nasal (−4 ± 9 μm) and superonasal (−4 ± 8 μm) meridians ($p < 0.05$) at 6 D. Although there was no main effect of eccentricity ($p = 0.857$), the accommodation-meridian-eccentricity interaction approached significance ($p = 0.068$). When the meridians were examined based on their annulus eccentricity, the temporal, inferotemporal and inferior meridians were the only ones to change

significantly across the entire 2.5 mm radius, and the magnitude of thinning in these meridians increased with greater eccentricity from the fovea (temporal meridian −6 ± 10 µm (1 mm annulus), −9 ± 13 µm (3 mm annulus), −13 ± 18 µm (5 mm annulus); inferotemporal meridian −5 ± 7 µm (1 mm), −7 ± 11 µm (3 mm), −10 ± 12 µm (5 mm); inferior meridian −5 ± 8 µm (1 mm), −7 ± 10 µm (3 mm), −7 ± 12 µm (5 mm)). Similar to the SFChT, the mean baseline parafoveal ChT across the full 5 mm was significantly different between refractive groups ($p < 0.05$), however when the change in parafoveal ChT with accommodation was examined, there was no significant effect of refractive group ($p = 0.352$).

Foveal RT was also found to decrease by a small but statistically significant degree with accommodation, with an average thinning of −0.7 ± 2 µm at the 3 D demand ($p < 0.05$) and −1.0 ± 2 µm at the 6 D demand ($p < 0.05$). There was no significant effect of refractive group on foveal RT, and there was no accommodation by refractive group interaction ($p > 0.05$). For all subjects with complete parafoveal data ($n = 35$) the mean RT also exhibited significant changes with accommodation ($p < 0.05$), with an average thinning of −1.0 ± 3 µm at 3 D, and −0.7 ± 3 µm at 6 D (Figure 5). However, only the change to the 3 D demand was significant ($p < 0.05$).

Analysis of the ocular biometry data for all subjects ($n = 40$) revealed a significant increase in corrected AL with accommodation ($p < 0.001$), with a mean elongation of +5 ± 11 µm during accommodation to the 3 D stimulus ($p < 0.05$), and +14 ± 13 µm for the 6 D stimulus ($p < 0.001$) (Figure 3, Table 2). The changes in AL with accommodation were not significantly different between myopes and emmetropes. As expected, the mean baseline AL for the myopes (24.89 ± 1 mm) was significantly greater than that of the emmetropic group (23.62 ± 0.8 mm) ($p < 0.05$). All subjects exhibited significant shallowing of the ACD and increase in the LT with

accommodation ($p < 0.001$), confirming the accommodative response. There were no significant differences in baseline ACD and LT between the emmetropic and myopic groups, and no significant differences in their change with accommodation. CCT was not affected by accommodation, and did not differ significantly between the refractive groups.

The OCT instrument's fine focus dial was used to focus the en-face retinal image to compensate for subject's refraction and accommodation, and could be used as a crude measure of the extent of accommodation. Using these values, the average accommodation response was 1.6 ± 0.5 D for the 3 D stimulus, and 4 ± 1 D for the 6 D stimulus. This estimate of accommodation response was significantly ($p < 0.001$) positively correlated with the change in ACD ($r = 0.781$) and significantly ($p < 0.001$) negatively correlated with the change in LT ($r = -0.798$), confirming that the accommodative response seen during biometry was consistent with the response seen during OCT measurements.

ANCOVA revealed that the changes in AL and SFChT exhibited a significant weak negative association ($p < 0.05$, $r^2 = 0.114$, slope $\beta = -0.155$) (Figure 3). The change in SFChT was positively correlated with the change in ACD ($p < 0.001$, $r^2 = 0.181$, slope $\beta = 0.015$) and negatively correlated with change in LT ($p < 0.001$, $r^2 = 0.183$, slope $\beta = -0.014$).

Discussion

This study provides the first assessment of the regional variations in the choroidal thinning response that accompanies accommodation in young adult myopes and

284 emmetropes. Using high resolution OCT imaging, we have shown that the most
285 prominent choroidal thinning occurs within the temporal meridian of the parafoveal
286 choroid, followed by the inferotemporal and then inferior meridians, with the
287 magnitude of thinning increasing with greater eccentricity from the fovea within this
288 quadrant. The magnitude of thinning observed in the temporal parafoveal choroid
289 with accommodation was ~200% greater than the subfoveal choroidal thinning. Both
290 the subfoveal and parafoveal choroidal thinning reached statistical significance only
291 at the highest levels of accommodation demand tested (6 D), indicating that the
292 choroidal thickness appears relatively stable during accommodation to demands of 3
293 D and less. A significant increase in AL was also observed, which was greatest at
294 the highest level of accommodation. These AL changes were significantly negatively
295 associated with the changes in the subfoveal choroid, but were of a greater
296 magnitude and in the opposite direction, with the magnitude of subfoveal choroidal
297 thinning on average accounting for 34% of the mean magnitude of axial elongation.
298 Despite using a different measurement method, the current results agree closely with
299 our previous findings using OLCR, which attributed 38% of the measured AL change
300 to thinning of the subfoveal choroid.[23] Although our previously reported changes in
301 ChT were slightly larger than those reported in this study, considering the axial
302 resolution of the different measurement techniques used (SD-OCT – 3.9 μm, and
303 OLCR[23] – 10-20 μm), the changes are comparable.

304 The asymmetry in the parafoveal choroidal thinning found in this study may provide
305 an insight into the potential mechanisms which underlie the change in choroidal
306 thickness during accommodation. While it has previously been suggested that the
307 centripetal force of ciliary muscle contraction during accommodation may cause a
308 mechanical stretching of the globe and subsequent axial elongation,[19-20] this seems

untenable as an explanation for our observed choroidal thinning. The connections between the anterior choroid and ciliary muscle tendons, coupled with the anterior movement of the ciliary muscle during contraction would be expected to cause a forward movement of the elastic fibres of the choriocapillaris at the posterior pole,[34-35] potentially thickening (rather than thinning) the posterior choroid.

Change in the autonomic tone of the eye associated with accommodation is a more likely mechanism to explain the regional choroidal thinning seen in this study. Since the ciliary body receives increased parasympathetic input during accommodation, it is possible that structures within the choroid that also receive autonomic input, such as the non-vascular smooth muscle (NVSM), may also receive this signal. This subpopulation of contractile cells within the choroid have been shown to contract in response to increased parasympathetic input, resulting in a subsequent thinning of the choroid,[34-36] leading to speculation that the NVSM plays a role in stabilising the fovea against any anterior movement caused by contraction of the ciliary muscle during accommodation.[37] The NVSM cells are most numerous in species with well-defined foveae,[38] and in humans are most often densely concentrated within the choroid in a 5-10 mm area extending from the temporal margin of the optic nerve, under the fovea, into the temporal retina.[37] The contraction of the NVSM network during accommodation may serve to counteract any forward movement of the choroidal elastic net, keeping the fovea in place and maintaining a clear image. Since these cells are reported to be most numerous within the temporal quadrant of the posterior pole, it follows that their contraction and resultant choroidal thinning during accommodation would be most pronounced within this region, as was found in this study.

Although the exact role of the intrinsic choroidal neurons (ICNs) remains unknown, like NVSM, they are most numerous in eyes with well-developed foveae and accommodation systems[39] and their distribution is skewed towards the central-temporal quadrant of the choroid.[40] Since the ICNs are found to be in close contact with the contractile NVSM cells, and receive a copy of the signal sent to the ciliary body during accommodation, it has been hypothesised that they are involved in the modulation of choroidal thickness to stabilise the foveal position during accommodation.[41]

Changes in the optics of the eye during accommodation could also potentially lead to fluctuations in ChT. Evidence from both animals[6, 7, 42] and humans[43-45] shows the choroid can rapidly modulate its thickness in response to retinal defocus. The estimate obtained from the OCT instrument's fine-focus dial indicated that on average our subjects probably exhibited an accommodative lag during the fixation task. This small hyperopic defocus could potentially trigger a thinning of the choroid, in the same manner reported in animal models. However, the relative asymmetry of the parafoveal choroidal thinning in this study is not consistent with the optical changes that typically accompany accommodation, the majority of which are rotationally symmetrical.[46-48] It should be noted though, that the exact pattern of defocus experienced by our subjects is not known since ocular aberrations were not measured in our study.

We observed a significant increase in AL after 10 minutes of accommodation in our young adult subjects, which was not significantly different between emmetropes and myopes. These findings show general agreement with previously published studies,[21, 23, 24] which reported increases in AL with accommodation, but no significant differences between the refractive groups. The increase we found in AL

was also of a much smaller magnitude than studies which did not take into account the accommodation induced error related to optical path length and refractive index that is present in commercial partial coherence interferometry instruments.[20] The changes in AL were negatively correlated with the changes in ChT, providing evidence that the changes in ChT and AL during accommodation may be mediated by the same mechanism.

The eye is reported to undergo a number of structural and functional changes as it ages, most notably through a progressive decline and loss of ability to accommodate.[49-50] The ciliary muscle reportedly thickens and adopts a more anterior-inward position[51-55] but appears to retain its contractile ability well into presbyopia,[52, 56-58] implicating that the age-related decline in accommodative ability is more likely lenticular in origin. The choroid is also known to undergo changes, with a decrease in thickness[9-10, 59-60] and a potential stiffening with age reported.[61] These involutional changes in the choroid and ciliary body structure may impact the distribution and magnitude of parafoveal choroidal thickness changes seen during accommodation in older age groups. Although our current study investigated these changes in young adults, it will be of interest for future research to examine pre-presbyopic or early-presbyopic individuals to observe how ageing changes to the uvea influence the accommodation induced choroidal thickness changes.

Although there was no significant difference in the magnitude of choroidal thinning with accommodation observed between the myopes and emmetropes in our study, the finding of short-term choroidal thinning associated with accommodation could still potentially have implications for human myopia and the role of near work in the development of myopia. In eyes that perform larger amounts of near work, the choroid will be thinned more frequently and for a greater period of time, which may

predispose the eye to longer term eye growth changes. From a clinical perspective, our findings provide an insight into the relative importance of accommodation control during fixation of internal instrument lights during OCT or biometry measurements of choroidal thickness. Given that our data shows that the subfoveal choroid does not thin significantly with up to 3 D of accommodation, small amounts of accommodation during fixation with OCT measurements will be unlikely to confound clinical choroidal measurements.

In conclusion, this study demonstrates that significant thinning of the choroid across the posterior pole, accompanies accommodation in a population of young adult myopes and emmetropes, with the largest magnitude changes occurring in the temporal and inferotemporal parafoveal choroidal regions. The regional distribution of the parafoveal choroidal thinning potentially provides an insight into the mechanisms underlying this change, as it overlaps with the documented distribution of the NVSM within the choroid.

Acknowledgements

The authors thank Mr Brett Davis for his assistance with the design and construction of the mounted Badal optometer and cold mirror system.

Disclosure: **E.C. Woodman-Pieterse**, None; **S.A. Read**, None; **M.J. Collins**, None; **D. Alonso-Caneiro**, None.

References

1. Grosvenor T, Scott R. Comparison of refractive components in youth-onset and early adult-onset myopia. *Optom Vis Sci* 1991;68:204-209.

2. Grosvenor T, Scott R. Three-year changes in refraction and its components in youth-onset and early adult-onset myopia. *Optom Vis Sci* 1993;70:677-683.

3. Jiang BC, Woessner WM. Vitreous chamber elongation is responsible for myopia development in a young adult. *Optom Vis Sci* 1996;73:231-234.

4. Ho M, Liu DTL, Chan VCK, Lam DSC. Choroidal thickness measurement in myopic eyes by enhanced depth optical coherence tomography. *Ophthalmology* 2013;120:1909-1914.

5. Read SA, Collins MJ, Vincent SJ, Alonso-Caneiro D. Choroidal thickness in myopic and nonmyopic children assessed with enhanced depth imaging optical coherence tomography. *Invest Ophthalmol Vis Sci* 2013;54:7578-7586.

6. Wallman J, Wildsoet C, Xu A, et al. Moving the retina: choroidal modulation of refractive state. *Vision Res* 1995;35:37-50.

7. Wildsoet C, Wallman J. Choroidal and scleral mechanisms of compensation for spectacle lenses in chicks. *Vision Res* 1995;35:1175-1194.

8. Fujiwara T, Imamura Y, Margolis R, Slakter JS, Spaide RF. Enhanced depth imaging optical coherence tomography of the choroid in highly myopic eyes. *Am J Ophthalmol* 2009;148:445-450.

9. Wei WB, Xu L, Jonas JB, et al. Subfoveal choroidal thickness: the Beijing eye study. *Ophthalmology* 2013;120:175-180.

10. Agawa T, Miura M, Ikuno Y, et al. Choroidal thickness measurement in healthy Japanese subjects by three-dimensional high-penetration optical coherence tomography. *Graefes Arch Clin Exp Ophthalmol* 2011;249:1485-1492.

11. Ouyang Y, Heussen FM, Mokwa N, et al. Spatial distribution of posterior pole choroidal thickness by spectral domain optical coherence tomography. *Invest Ophthalmol Vis Sci* 2011;52:7019-7026.

12. Curtin BJ. *The Myopias: Basic Science and Clinical Management*. Philadelphia: Harper & Row; 1985.

13. McBrien NA, Adams DW. A longitudinal investigation of adult-onset and adult-progression of myopia in an occupational group. Refractive and biometric findings. *Invest Ophthalmol Vis Sci* 1997;38:321-333.

14. Jacobsen N, Jensen H, Goldschmidt E. Does the level of physical activity in university students influence development and progression of myopia? A 2-year prospective cohort study. *Invest Ophthalmol Vis Sci* 2008;49:1322-1327.

15. Onal S, Toker E, Akingol Z, et al. Refractive errors of medical students in Turkey: one year follow-up of refraction and biometry. *Optom Vis Sci* 2007;84:175-180.

16. Ip JM, Saw SM, Rose KA, et al. Role of near work in myopia: findings in a sample of Australian school children. *Invest Ophthalmol Vis Sci* 2008;49:2903-2910.

17. Saw SM, Cheng A, Fong A, Gazzard G, Tan DT, Morgan I. School grades and myopia. *Ophthalmic Physiol Opt* 2007;27:126-129.

18. Ostrin L, Kasthurirangan S, Win-Hall D, Glasser A. Simultaneous measurements of refraction and A-scan biometry during accommodation in humans. *Optom Vis Sci* 2006;83:657-665.

19. Drexler W, Findl O, Schmetterer L, Hitzenberger CK, Fercher AF. Eye elongation during accommodation in humans: differences between emmetropes and myopes. *Invest Ophthalmol Vis Sci* 1998;39:2140-2147.

20. Mallen EA, Kashyap P, Hampson KM. Transient axial length change during the accommodation response in young adults. *Invest Ophthalmol Vis Sci* 2006;47:1251-1254.

21. Read SA, Collins MJ, Woodman EC, Cheong SH. Axial length changes during accommodation in myopes and emmetropes. *Optom Vis Sci* 2010;87:656-662.

22. Woodman EC, Read SA, Collins MJ, et al. Axial elongation following prolonged near work in myopes and emmetropes. *Br J Ophthalmol* 2011;95:652-656.

23. Woodman EC, Read SA, Collins MJ. Axial length and choroidal thickness changes accompanying prolonged accommodation in myopes and emmetropes. *Vision Res* 2012;72:34-41.

24. Zhong J, Tao A, Xu Z, et al. Whole eye axial biometry during accommodation using ultra-long scan depth optical coherence tomography. *Am J Ophthalmol* 2014;157:1064-1069.

25. Sizmaz S, Küçükerdönmez C, Pinarci E, Karalezli A, Canan H, Yilmaz G. The effect of smoking on choroidal thickness measured by optical coherence tomography. *Br J Ophthalmol* 2013;97:601-604.

26. Spaide RF, Koizumi H, Pozzoni MC. Enhanced depth imaging spectral-domain optical coherence tomography. *Am J Ophthalmol* 2008;146:496-500.

27. Brown JS, Flitcroft DI, Ying GS, et al. In vivo human choroidal thickness measurements: evidence for diurnal fluctuations. *Invest Ophthalmol Vis Sci* 2009;50:5-12.

28. Chakraborty R, Read SA, Collins MJ. Diurnal variations in axial length, choroidal thickness, intraocular pressure, and ocular biometrics. *Invest Ophthalmol Vis Sci* 2011;52:5121-5129.

29. Read SA, Collins MJ, Iskander DR. Diurnal variation of axial length, intraocular pressure, and anterior eye biometrics. *Invest Ophthalmol Vis Sci* 2008;49:2911-2918.

30. Alonso-Caneiro D, Read SA, Collins MJ. Automatic segmentation of choroidal thickness in optical coherence tomography. *Biomed Opt Express* 2013;4:2795-2812.

31. Bland JM, Altman DG. Statistical methods for assessing agreement between two methods of clinical measurement. *Lancet* 1986;327:307-310.

32. Atchison DA, Smith G. Possible errors in determining axial length changes during accommodation with the IOLMaster. *Optom Vis Sci* 2004;81:283-286.

33. Bland JM, Altman DG. Calculating correlation coefficients with repeated observations: part 1 - correlation within subjects *Br Med J* 1995;310:446.

34. Flügel-Koch C, May CA, Lütjen-Drecoll E. Presence of a contractile cell network in the human choroid. *Ophthalmologica* 1996;210:296-302.

35. Poukens V, Glasgow BJ, Demer JL. Nonvascular contractile cells in sclera and choroid of humans and monkeys. *Invest Ophthalmol Vis Sci* 1998;39:1765-1774.

36. Meriney SD, Pilar G. Cholinergic innervation of the smooth muscle cells in the choroid coat of the chick eye and its development. *J Neurosci* 1987;7:3827-3839.

37. May CA. Non-vascular smooth muscle cells in the human choroid: distribution, development and further characterization. *J Anat* 2005;207:381-390.

38. May CA. Nonvascular smooth muscle alpha-actin positive cells in the choroid of higher primates. *Curr Eye Res* 2003;27:1-6.

39. Flügel-Koch C, Kaufman PL, Lütjen-Drecoll E. Association of a choroidal ganglion cell plexus with the fovea centralis. *Invest Ophthalmol Vis Sci* 1994;35:4268-4272.

40. Flügel C, Tamm ER, Mayer B, Lütjen-Drecoll E. Species differences in choroidal vasodilative innervation: evidence for specific intrinsic nitrergic and VIP-positive neurons in the human eye. *Invest Ophthalmol Vis Sci* 1994;35:592-599.

41. Schrödl F, De Laet A, Tassignon MJ, et al. Intrinsic choroidal neurons in the human eye: projections, targets, and basic electrophysiological data. Invest Ophthalmol Vis Sci 2003;44:3705-3712.

42. Zhu X, Park TW, Winnawer J, Wallman J. In a matter of minutes, the eye can know which way to grow. *Invest Ophthalmol Vis Sci* 2005;46:2238-2241.

43. Read SA, Collins MJ, Sander BP. Human optical axial length and defocus. *Invest Ophthalmol Vis Sci* 2010;51:6262-6269.

44. Chakraborty R, Read SA, Collins MJ. Monocular myopic defocus and daily changes in axial length and choroidal thickness of human eyes. *Exp Eye Res* 2012;103:47-54.

45. Chakraborty R, Read SA, Collins MJ. Hyperopic defocus and diurnal changes in human choroid and axial length. *Optom Vis Sci* 2013;90:1187-1198.

46. Atchison DA, Collins MJ, Wildsoet CF, Christensen J, Waterworth MD. Measurement of monochromatic ocular aberrations of human eyes as a function of accommodation by the Howland aberroscope technique. *Vision Res* 1995;35:313-323.

47. Cheng H, Barnett JK, Vilupuru AS, Marsack JD, Kasthurirangan S, Applegate RA, Roorda A. A population study on changes in wave aberrations with accommodation. *J Vis* 2004;4:272-280.

48. Atchison DA, Collins MJ, Wildsoet CF, Christensen J, Waterworth MD. Measurement of monochromatic ocular aberrations of human eyes as a function of

526 accommodation by the Howland aberroscope technique. *Vision Res* 1995;35:313-
527 323.
528 49. Atchison DA. Accommodation and presbyopia. *Ophthalmic Physiol Opt*
529 1995;15:255-272.
530 50. Gilmartin B, The aetiology of presbyopia: a summary of the role of lenticular
531 and extralenticular structures. *Ophthalmic Physiol Opt* 1995;15:431-437.
532 51. Pardue MT, Sivak JG. Age-related changes in human ciliary muscle. *Optom*
533 *Vis Sci* 2000;77:204-210.
534 52. Sheppard AL, Davies LN. The effect of ageing on in vivo human ciliary muscle
535 morphology and contractility. Invest Ophthalmol Vis Sci 2011;52:1809-1816.
536 53. Strenk SA, Strenk LM, Guo S. Magnetic resonance imaging of aging,
537 accommodating, phakic, and pseudophakic ciliary muscle diameters. *J Cataract*
538 *Refract Surg* 2006;32:1792-1798.
539 54. Strenk SA, Strenk LM, Guo S. Magnetic resonance imaging of the
540 anteroposterior position and thickness of the aging, accommodating, phakic and
541 pseudophakic ciliary muscle. *J Cataract Refract Surg* 2010;36:235-241.
542 55. Tamm S, Tamm E, Rohen JW. Age-related changes of the human ciliary
543 muscle. A quantitative morphometric study. *Mech Ageing Dev* 1992;62:209-221.
544 56. Croft MA, Glasser A, Heatley G, et al. Accommodative ciliary body and lens
545 function in rhesus monkeys, I: normal lens, zonule and ciliary process configuration
546 in the iridectomized eye. *Invest Ophthalmol Vis Sci* 2006;47:1076-1086.
547 57. Croft MA, Glasser A, Heatley G, et al. The zonula, lens, and circumlental
548 space in the normal iridectomised rhesus monkey eye. *Invest Ophthalmol Vis Sci*
549 2006;47:1087-1095.

550 58. Glasser A, Kaufman PL. The mechanism of accommodation in primates.
551 *Ophthalmology* 1999;106:863-872.
552 59. Margolis R, Spaide RF. A pilot study of enhanced depth imaging optical
553 coherence tomography of the choroid in normal eyes. *Am J Ophthalmol*
554 2009;147:811-815.
555 60. McCourt EA, Cadena BC, Barnett CJ, Ciardella AP, Mandava N, Kahook MY.
556 Measurement of subfoveal choroidal thickness using spectral domain optical
557 coherence tomography. *Ophthalmic Surg Lasers Imaging* 2010;41:S28-33.
558 61. Ugarte M, Hussain AA, Marshall J. An experimental study of the elastic
559 properties of the human Bruch's membrane-choroid complex: relevance to ageing.
560 *Br J Ophthalmol* 2006;90:621-626.

Figures

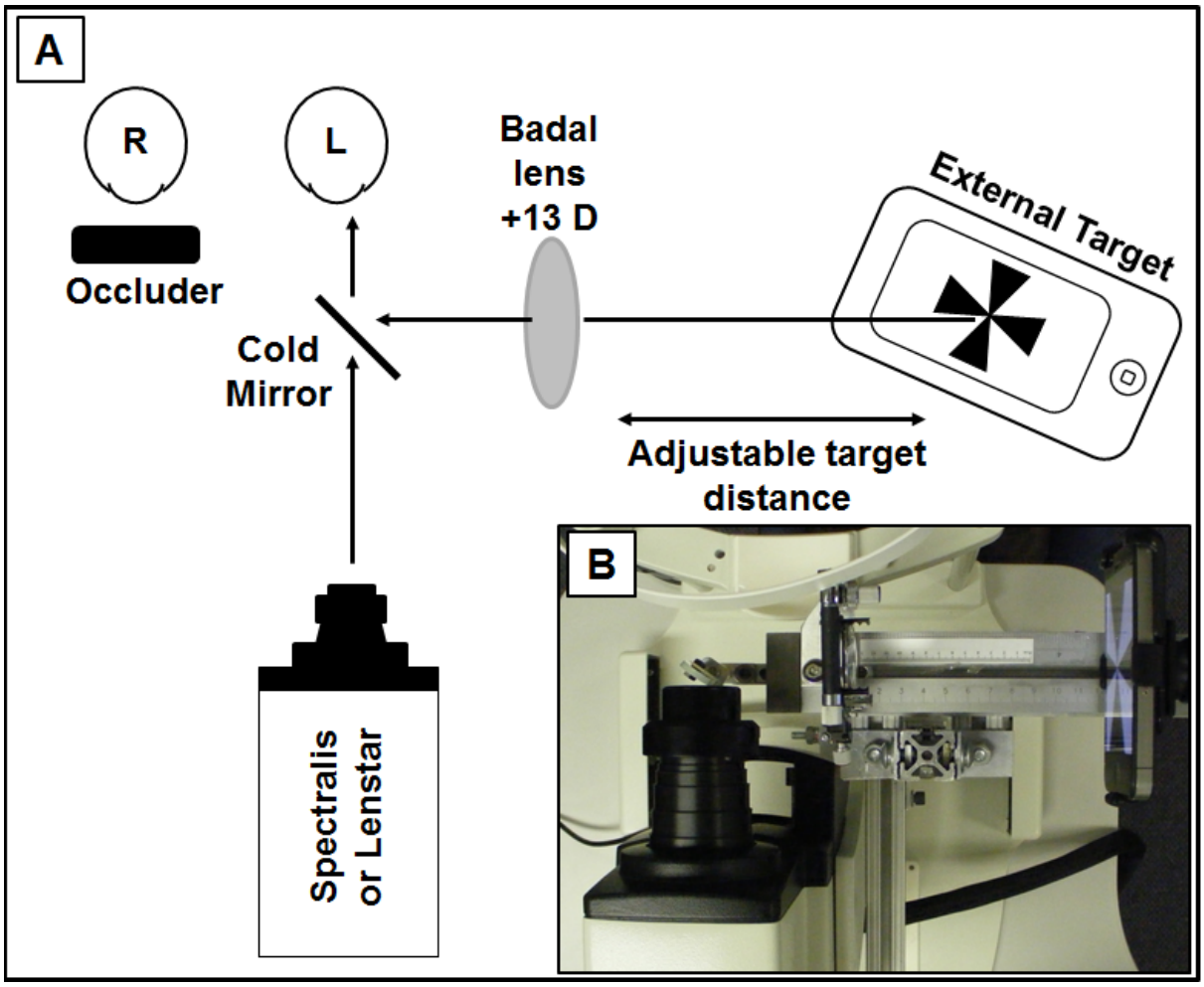

Figure 1. A) Aerial schematic of the Badal optometer and cold mirror system mounted before the Spectralis SD-OCT and Lenstar biometer. The subject's left eye was measured while they viewed a Maltese cross displayed on an LCD screen through a cold mirror imaged through a +13 D Badal optometer. This allowed for the correction of the subject's ametropia, and to provide accommodation stimuli of 0, 3 and 6 D. The right eye was occluded. B) Aerial image of Badal optometer/cold mirror system mounted before the Spectralis SD-OCT.

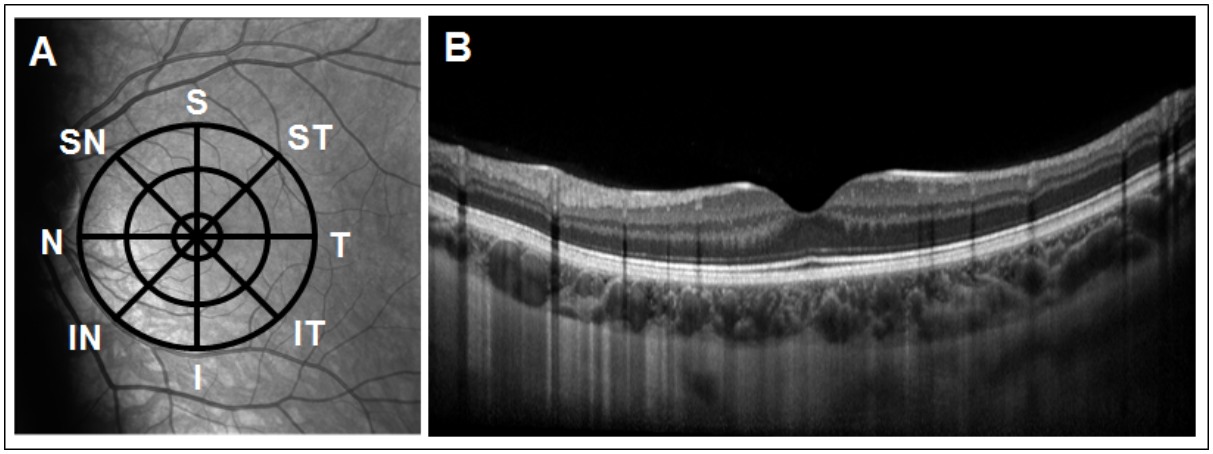

Figure 2. A) An example of a typical en-face image obtained from the OCT with the cold mirror in place, overlayed with the meridians (S – superior, I – inferior, N – nasal, T – temporal, SN – superonasal, ST – superotemporal, IN – inferonasal, IT – inferotemporal) and concentric annuli (diameter of 1, 3 and 5 mm, centred on the fovea) used for analysis of the parafoveal ChT and RT data. The shadow cast on the nasal retina and optic nerve head is from the edge of the cold mirror. B) An example of a typical averaged B-scan from the OCT with the cold mirror in place.

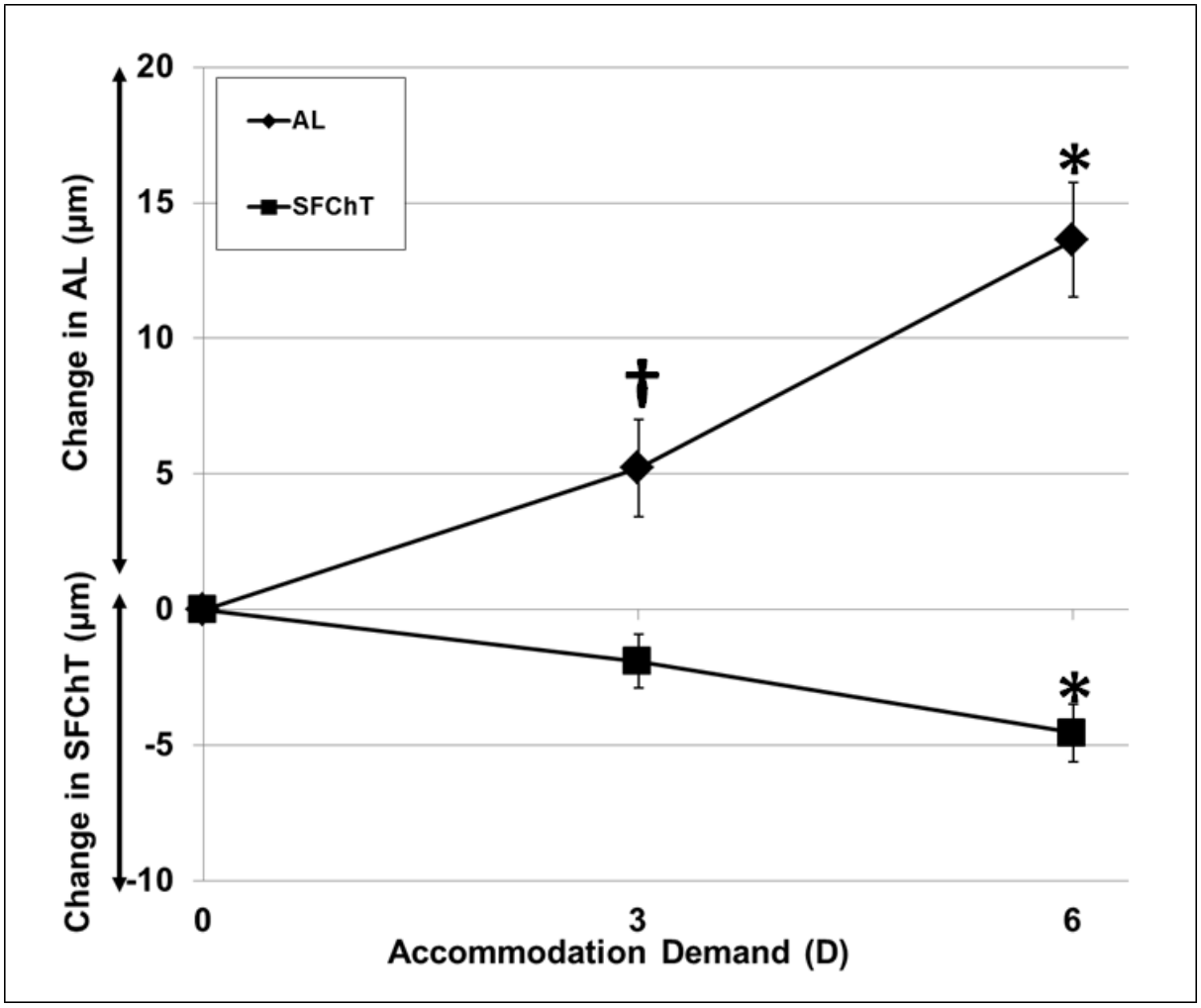

578

579 Figure 3. Change in AL and SFChT (mean ± SEM µm) from baseline with
580 accommodation in all subjects (*n* = 40). The asterisks (*) indicate a highly significant
581 change from baseline ($p < 0.001$), and the cross (†) indicates a significant change
582 from baseline ($p < 0.05$).

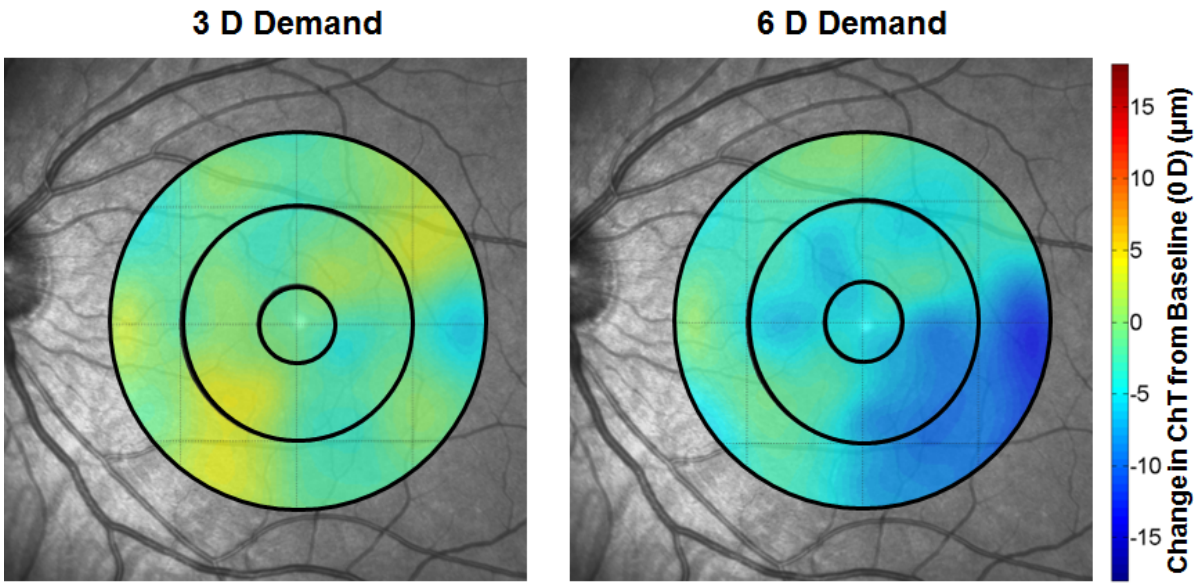

583

584 Figure 4. Maps illustrating the mean change in ChT (µm) with accommodation
585 demand (3 and 6 D) from baseline (0 D) across the central 5 mm of the macula for
586 all subjects with valid parafoveal data (*n* = 35). Negative values indicate a thinning
587 of the choroid with accommodation. Circles illustrate the 3 concentric annuli (of 1, 3
588 and 5 mm diameter) used in the analysis.

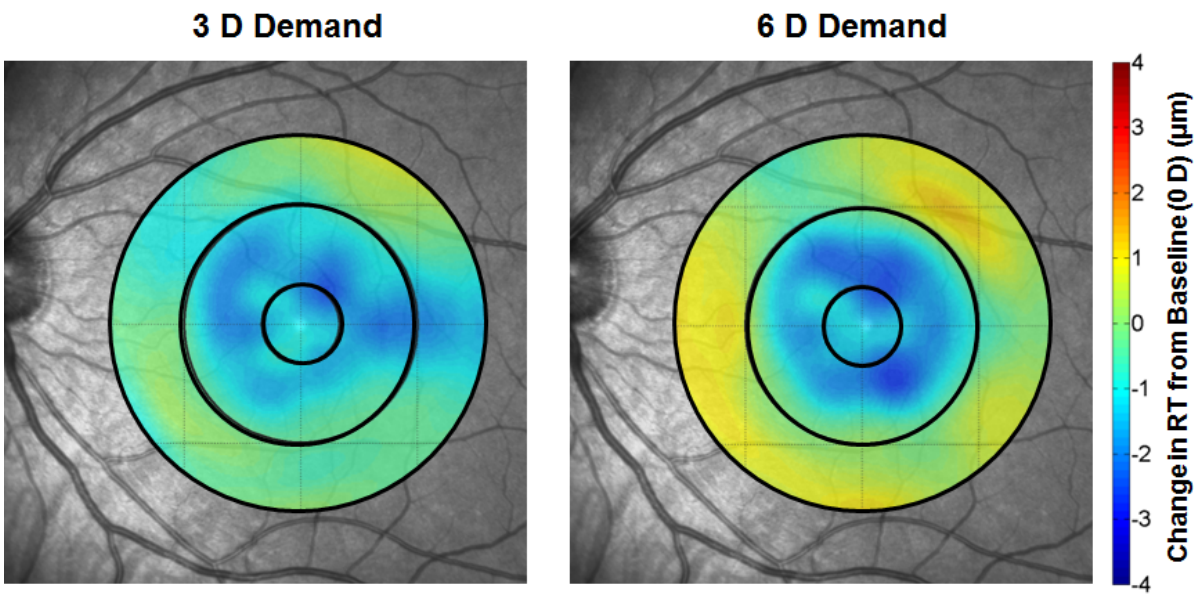

589

590 Figure 5. Maps of the mean change in RT (µm) with accommodation demand (3 and
591 6 D) from baseline (0 D) across the central 5 mm of the macular for all subjects (*n* =
592 35). Negative values indicate a thinning of the retina with accommodation. Circles
593 illustrate the 3 concentric annuli (of 1, 3 and 5 mm diameter) used in the analysis.

594

Tables

Table 1. Mean (± SD) baseline (BL), and changes in parafoveal ChT from baseline with accommodation to 3 D and 6 D stimuli for each meridian. For Δ 3 D and Δ 6 D, a positive change indicates a thickening of the choroid, and a negative change indicates a thinning of the choroid.

Meridian	BL (μm)	Δ 3 D (μm)	Δ 6 D (μm)
Superior	335 ± 69	−2 ± 13	−3 ± 11
Superotemporal	333 ± 66	1 ± 13	−3 ± 9
Temporal	330 ± 70	−3 ± 9	−9 ± 12*
Inferotemporal	328 ± 73	−2 ± 8	−8 ± 8*
Inferior	326 ± 75	−2 ± 9	−6 ± 8*
Inferonasal	300 ± 75	1 ± 12	−3 ± 12
Nasal	281 ± 86	0 ± 6	−4 ± 9†
Superonasal	307 ± 74	−1 ± 8	−4 ± 8†

*Indicates a highly significant change from baseline ($p < 0.001$)

†Indicates a significant change from baseline ($p < 0.05$)

Table 2. Mean (± SD) ocular biometric data at baseline (BL, 0 D) and their changes with accommodation to 3 D and 6 D stimuli. For Δ 3 D and Δ 6 D, a positive change indicates a thickening and a negative change indicates a thinning.

		CCT (μm)	ACD (mm)	LT (mm)	AL (mm/Δ μm)
All Subjects (*n* = 40)	**BL**	542 ± 33	3.22 ± 0.3	3.47 ± 0.2	24.25 ± 1
	Δ 3 D	−0.7 ± 2	−0.09 ± 0.05*	0.10 ± 0.05*	5 ± 11†
	Δ 6 D	−0.2 ± 2	−0.28 ± 0.06*	0.29 ± 0.07*	14 ± 13*
Emmetropes (*n* = 20)	**BL**	544 ± 29	3.18 ± 0.3	3.47 ± 0.2	23.62 ± 0.8
	Δ 3 D	−0.5 ± 2	−0.10 ± 0.05*	0.11 ± 0.05*	3 ± 11
	Δ 6 D	0.2 ± 2	−0.29 ± 0.06*	0.30 ± 0.07*	13 ± 15
Myopes (*n* = 20)	**BL**	539 ± 38	3.26 ± 0.3	3.47 ± 0.2	24.89 ± 1
	Δ 3 D	−0.9 ± 3	−0.08 ± 0.04*	0.09 ± 0.05*	7 ± 12
	Δ 6 D	0 ± 2	−0.27 ± 0.06*	0.28 ± 0.07*	15 ± 12

*Indicates a highly significant change from baseline ($p < 0.001$)

†Indicates a significant change from baseline ($p < 0.05$)